Strathprints Institutional Repository

Attya, A. B. and Subramanian, B. (2015) Impact of wind farms capacity factor and participation in frequency support – reliability analysis. In: IEEE 5th International conference on Power Engineering, Energy and Electrical Drives,, 2015-05-11 - 2015-05-13. , http://dx.doi.org/10.1109/PowerEng.2015.7266294

This version is available at http://strathprints.strath.ac.uk/55057/

Impact of Wind Farms Capacity Factor and Participation in Frequency Support – Reliability Analysis

A. B. Attya
Department of Electronic and Electrical Engineering
University of Strathclyde
ayman.attya@strath.ac.uk

B. Subramanian
Department of Electrical Engineering and Information Technology
Technical University of Darmstadt

Abstract— expanded integration of wind energy implies technical confronts to maintain system reliability. Thus, comprehensive reliability models for wind turbines and related features are required. Composite and precise wind farms (WFs) reliability analysis includes wind turbine generator (WTG) detailed models besides wind speed (WS) probabilistic variations considering wake effects. This paper is considered as an extension to the proposed multi-state duration sampling model to asses WTG reliability integrated with a comprehensive representation for WF [1]. The paper investigates the impacts of two WTG frequency support operation algorithms on capacity factors and first hierarchical level indices. LOEE is evaluated using a novel method to emphasis the chronological coordination between load and WS attitudes. System and load points' reliability indices are estimated at moderate penetration levels of wind energy using a simplified technique. Results insure the feasibility of the composite WTG reliability model and provide reasonable indicators for WFs integration influence.

Keywords-Wind power, reliability, frequency support, Monte Carlo simulation

I. INTRODUCTION

Renewable energies continue to make a strong foothold to contribute to the rapidly rising share of energy supply in this decade with wind power accounting for 39% from the integrated capacity in 2012 [2]. Independent organizations and governmental bodies have instilled the enforcement of a well-developed framework to secure energy supply by allowing high levels of wind power penetration in the next years. Multiple investigations on WFs reliability assessment have been conducted. Research work [3, 4] focused on the development of a reliability schema for WFs and composite power systems. Literatures made use of WS models but commonly implied the basic Jensen model for wind streams propagation [2]. Kim and Singh applied the Markov model to simulate WSs dynamics [5], and the pitfalls of using this model are addressed in [6]. The participation of WTGs and WFs in frequency drops mitigation is the second topic involved in this paper. System operators (SOs) face problems during frequency dips, because the traditional primary and secondary responses scenarios could not be applied by WFs. As an illustration, conventional plants respond easily and efficiently to deviations by controlling the output active power using governors [7]. This return to the stable and controllable amounts of fossil fuels burnt to provide steam to the turbine, and in turn the mechanical power running generator shaft. On the contrary, WS is neither controlled nor expected with high accuracy. Researchers offered several algorithms to make WTGs and WFs capable of supporting the system, during frequency events [8]. Attya and et el. proposed

algorithms which make WTG able to mitigate frequency excursion or nearly neutralizes the negative influence of WS intermittency during frequency excursions [9, 10]. For this aim, WTGs are not operated based on maximum power tracking (MPT [11]) but other speed and/or power control methods. WTG de-loading technique is highlighted in [12], such that WTG output power is reduced by certain percentage; hence the frequency support is insured by the deficit between optimum and de-loaded power values. Further strategy is presented in [13], where pitch angle control is utilized to keep WT output de-loaded to a predetermined reference. Completely different point of view rejects any de-loading or reduction in WFs output, but it counts on energy storage mediums. Wide range of energy storage facilities are discussed in literature, mainly, hydro pumping stations, batteries banks and flywheels. Nevertheless, economic constrains halt the expansion of storage solutions, especially, batteries.

WF capacity factor (CF) is considered the nexus between the two previously mentioned topics. As an illustration, the retired conventional capacities which are replaced by WFs have a great impact on the post balance between generation and load demand (i.e., imbalance is the main cause for frequency drops [14]). Thus, it is mandatory to find an accurate method to assess CF, and at the same time acknowledges the reliability impact. In the light of previous survey, this paper investigates the impact of conventional generation replacement by WFs on selected reliability indices. The capacities of displaced conventional units are decided based on the estimated CFs. LOEE index is evaluated using a modified method to insure the chronological synchronization between load demand attitude and WSs. The influence of the implied WTG operation method (i.e. integrated WTG power curve, for example MPT or de-loaded operation for possible frequency support) is acknowledged. Thus, the highlighted operation methods are compared from reliability and CF point of views.

II. THEORETICAL BACKGROUND

A. WTG and WF reliability

WTG is a collection of an estimated 8,000 components out of which ten main components play a crucial role in determining the overall functioning and performance of WTG [7]. The ten components are designated under two groups namely Critical and Non-critical in accordance to their contribution in the failure of WTG. The Critical group includes; tower, pitch control and blades, gearbox, generator, converters, control system and transformer. A failure of one of these components switches the WTG to the downstate. Thus, these components are assigned an equal high priority level. On the other side,

Non-critical group constitutes the yaw system, brake system and sensors [6]. Failure of one or more of non-critical components results in a de-rated operation (e.g., 70% from WTG rated power). Each of these components causes different de-rating factor when it fails.

The WF reliability is involved with other components, for example, substation(s) equipment and internal cables. However, the inclusion of these components exerts huge additional computational and time burdens. Meanwhile, its influence on wind energy reliability assessment is minor [15]. Conversely, WS forecasting mechanisms are effective, especially when the reliability indices counting on harvested energy are estimated. Moreover, it is relevant to estimate the WS magnitude incident on each WTG according to its position with respect to the WF layout and WTGs geographical distribution.

B. WTG operation method

This subsection explains briefly WTG operation in de-loading and the authors published proposed algorithm (it will be called now on "partial de-loading") [10].

1) De-loading operation

WTG is operated such that its output power is always less than the optimum available power by a certain predefined ratio or absolute value. Thus, the deficit between the actual output power and optimum one is a strategic reserve to support the system during frequency drops. De-loading could be applied by two methods:

- Running WTG at rotational speed higher than the optimum speed. This method is called WT over-speeding which is valid for variable speed WTGs.
- Continuous activation of pitch control so that the output power is reduced based on the implied pitch angle. This technique is applicable for any WTG equipped with pitch angle controls [11].

In both methods a predefined de-loading factor (D_F) is selected according to the target WTGs contribution in frequency drops mitigation. D_F numerical value is adjusted based on several givens including the level of WFs penetration and the history of frequency excursions in the system. In this paper, $D_F = 15\%$.

2) Partial de-loading algorithm

The major merits and uniqueness of this algorithm lie in three points; 1) It correlates between WTG type and WS conditions in the WF location, 2) The de-loading is activated only within certain range of WS which is determined based on certain procedure. 3) Its capability to handle WS drops intersecting with frequency events, reducing possible negative consequences. The first step is to evaluate the pivot three parameters of proposed algorithm, namely, 1) base rotational speed, 2) base WS (WS_B) and 3) low WS (WS_{low}) [10].

The proposed algorithm operates WTG in de-loaded operation within the WS range ($WS_{low} < WS < WS_R$) using pitch angle control. It is worth mentioning that when WS exceeds WS_B by certain margin, rotor speed is allowed to accelerate above its base value, hence higher output is guaranteed. When output reaches its rated value (i.e., 1 p.u.) the de-loading is deactivated to utilize all the available wind energy. However, supporting the system, in case of frequency excursions is achieved by overloading the WTG for a predefined duration. When instantaneous WS drops, kinetic energy is extracted from WT

rotating parts by fixing the former output and decelerating rotor speed to a new speed which avoids loss of synchronism. In words, de-loading is applied at the following conditions: 1) $WS_{low} < WS < WS_R$ and 2) normal output is less than 1 p.u. Further details about this algorithm are not prerequisites to comprehend offered reliability analysis.

3) Manufacturer power curve

WTG fabricating companies provide standard power curves for each WTG type where the expected output power at each WS is indicated within the margin between cut-in and cut-out WSs. These values are based on continuous monitoring for WTG performance where the average value of several records at the same WS is considered. MPT can be manipulated into a lookup table with appropriate interpolation method; hence optimum output is obtained at any WS. The most critical region of this curve is between cut-in and rated WSs, elsewhere the output is either rated or zero. Operating WTG in MPT mode cancels any contribution for the WTG in frequency drops curtailment. Further illustrating figures comparing between the three algorithms are shown in Subsection IV. For further details please refer to [16].

III. Integrated Reliability Assessment Algorithms

Subsections A and B summarize the method proposed in [1].

A. WTG reliability

A two-state operation cycle based on state duration sampling is used to obtain an artificial operating history of WTG components. The failure and the repair rates (λ and μ respectively) of each component are assumed to be exponentially distributed for calculating the Time to Fail (TTF) and Time to Repair (TTR) using (1). Aggregate values for λ and μ are estimated for critical group components using method of series-component reliability [17]. Since the failure of one of Critical components leads to complete breakdown. Each Non-critical component is considered as a single group while all Critical components are aggregated in one group. As an illustration, a Non-critical component, during its down state, has a different impact on WTG output where a de-rated percentage is given with respect to component priority. De-rating factors caused by each non-critical component are 25, 15 and 5% for Sensors, Yaw system and Brake system respectively. In conclusion, nine states (seven of them are de-rated) are defined for WTG. Obtained curves are timely added to get the WTG transition multi-state array (i.e., Availability).

$$TTF = -1/\lambda \cdot \ln(R), \quad TTR = -1/\mu \cdot \ln(R') \qquad (1)$$

B. WF layout and reliability

1) WTGs positioning, WS forecasting and propagation

WTGs are uniformly distributed across WFs' terrains for simplicity and acknowledging the almost flat ground of the candidate locations to host WFs in Egypt. In other words, the WFs borders length and width are equally sectionalized to keep a fixed distance between any two neighbor WTGs, namely, six times the rotor diameter (d) of installed WTG type [18]. Each WF is composed of one type of WTGs distributed in regular rows so that all rows have equal number of WTGs.

WS data are available for all locations in the form of time series average readings in 10 minutes resolution for 1 year. However,

the proposed analysis accuracy is improved by generating different WSs arrays, for each simulation sample, with 15 minutes resolution through Wei-bull distribution using (2) where α and β are the shape and scale parameters respectively. A vector y consisting of uniformly distributed random numbers in the range (0, 1) are simulated and applied to the transformation function to obtain the WS array for the desired simulation period.

$$W(y) = \alpha \cdot \beta \cdot y^{\beta-1} \cdot \exp(-\alpha y^{\beta}) \quad (2)$$

The wake effect produced by the propagation of wind streams is also considered. The upstream WS at each WTG is estimated using (3) where WS_o and WS_x are the upstream WS magnitudes at the previous WTG and the next one respectively. Thrust coefficient (C_T) equals $7/WS_o$ and k is 0.075 for onshore WTGs [19]. The distance at which the wake WS is calculated is 'x' (i.e., x = 6*d) depending on WTG size. WS stream direction is always perpendicular on WF rows. Hence, for simplicity, the WS incident on the WTGs of the same row is typical and it is evaluated using (3). The time delay consumed by wind stream to cover the separating distance between each two successive rows is WS_x/x.

$$WS_x = WS_o \left[\left(1 - \left(1 - \sqrt{(1-C_T)} \right) \right) \cdot \left(\frac{d}{d + 2 \cdot k \cdot x} \right) \right] \quad (3)$$

C. Impact of WTG Operation method

The power curve of each WTG type is integrated to evaluate the output power at any WS. Three different operation methods are investigated as explained earlier in Section II.B. However, in case of continuous de-loading, MTTF of pitching and converter subsystems are reduced by 15%. This assumption reflects the nature of this operation method which imposes intensive variations for rotor speed and pitch angle leading to higher failure rate for the responsible components. Meanwhile, partial de-loading reduces MTTF by 8% since de-loading is not continuous. Generally, operation method mainly affects the amounts of harvested wind energy.

D. Simulation sequence

The following steps describe briefly how the proposed algorithms are simulated using MATLAB and Simulink.
- Generate the initial incident WS time series in the considered WF within T. The actual chronological WSs data in concerned location are processed through (4).
- For each row (i), generate the state transition chronological arrays of installed WTGs. Keep in mind that, WTGs in the same row face the typical WS as explained at the end of subsection B. Hence, aggregate state array of a row (State$_{row-i}$) is the summation of all WTG arrays in this row.
- Repeat for all WF rows (number of rows/WF is N_{Row}).
- Repeat for all WFs.
- Run a Simulink model to generate: a) WS time series arrays incident on each row, in each WF, acknowledging wake effect, hence, b) output power array of a single WTG in row (i) is obtained based on the applied operation method look-up table (P_{row-i}).
- Evaluate WF availability and output time arrays using (4) and (5) resp., where N_{WTG} is the number of WTG in the WF.

- Repeat previous steps for 'N_S' samples until the error stopping criteria of Monte Carlo method is achieved.

$$WF_{availability} = \frac{\sum_{i=1}^{N_{Row}} State_{row-i}}{N_{WTG}} \quad (4)$$

$$WF_{o/p} = \sum_{i=1}^{N_{Row}} (State_{row-i} \cdot P_{row-i}) \quad (5)$$

IV. CASE STUDY

Proposed algorithms are applied on 12 different locations which are candidates to host WFs. Due to lack of geographical information; it is assumed that all WFs have the same terrain area, namely, 50 km^2 in analogy to Za'afrana WF which is already constructed [24]. Three different WTGs types are installed; N-117, E-101 and G-90 whose main characteristics are depicted in Table I and the Partial de-loading power curves are obtained [10, 16]. The selection of WTG type for each location is based on [14]. As explained in Subsection III.B, N_{WTG} counts on WF terrain dimensions and d. Since all WFs have the same area thus, every type has equal N_{WTG} in all locations. Moreover, each WF is divided into 6 to 8 rows facing wind streams (14 to 16 WTGs/row). Types and numbers of installed WTGs in each WF, and WF fixed layout are in Fig. 1. The failure and repair rates of integrated WTGs types are not published by their vendors. Thus, standard reliability data for WTG components given in Table II [6] are assigned for G-90. Meanwhile, the reliability data of the other two types are proportional to their rotor diameter. For example, standard tower MTTR is 104 hours then G-90 tower has same value, while N-117 scaled value is 104*117/90. This simplified criterion assumed that larger WTGs require more reliable components, but failures take longer time to be fixed due to larger size complications.

V. CAPACITY FACTOR ASSESSMENT

The CFs for the 12 WFs is estimated through Monte Carlo simulation method as in [1]. The CF values for several locations with the integration of the three investigated operation methods are depicted in Fig. 2. The evaluated CFs show great variation mainly based on WS conditions in each location. The locations characterized with high average WS (e.g., NW and Ras Ghareb) CF is about 60%.
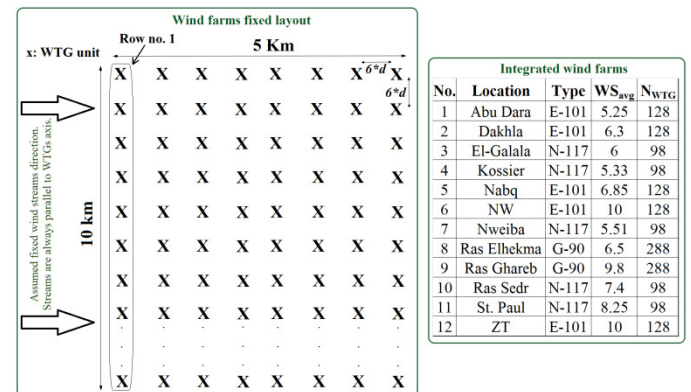

Figure 1 Implemented fixed WF layout (for wake estimation purposes), and the WTGs types and numbers for each WF

Conversely, lowest CF is achieved by Kossier with 24% which is still in the acceptable worth limits. On the other hand, the operation algorithm causes slight deviations in the estimated CF. However; the locations of better WS conditions have larger gaps between different algorithms. For example, Ras Ghareb location has showed a 9% deficit between MPT and de-loaded operation. Meanwhile, partial de-loaded method mitigated energy loss by 4% which is considerable value (202 GWh/year). The partial de-loaded algorithm proves superiority over de-loaded method in most of locations. Nevertheless, locations of poor WS conditions (i.e., average WS is dramatically less than WTG rated WS) have a minor deficit for the favor of de-loaded algorithm. As an illustration, the operation of WTG at base rotational speed, which deviates from optimum speed sometimes especially at very low WS, waste more energy compared to de-loaded operation. Moreover, the durations of rated WTG operation in such locations are mitigated. Thus, the advantage of partial de-loading which avoids de-loading at rated output is lost. It is worth mentioning that lower reliability levels of some components in de-loaded operation alleviate the difference between the two frequency support algorithms in poor WS locations. In addition, higher N_{WTG} increases failure probability which aggravate the WF availability but the other positive factors overcome this point.

VI. WIND ENERGY IMPACT ON SYSTEM RELIABILITY

A. Case studies

Estimated CFs in the previous section are utilized to decide the number and location of the conventional units which are forced to retire. In other words, planned WFs replace certain conventional capacity. Replacement procedure focused on conventional plants which are geographically near from intended WFs sites (i.e. WFs are integrated to the present network without the assessment of possible expansions). The Egyptian grid composite layout is presented in Fig. 3 before and after WFs integration. Steam generation participates with 76% from the total generation capacity. The average annual load demand was 12.25 GW in 2010 based on hourly records. The failure and repair rates for all conventional units, about 186 units, are provided by the concerned authorities.

TABLE I.   INTEGRATED WTG TYPES MAJOR SPECIFICATIONS

WT type	G-90	E-101	N-117
d, m	90	101	117
Cut-in WS, m/s	3	3	3
Cut-out WS, m/s	21	28	20
Rated WS, m/s	16	13	11
Rotor speed, r. / s	0.94 - 1.99	0.67 - 2.31	1.19 - 2.1

TABLE II.   STANDARD WTG COMPONENTS RELIABILITY DATA

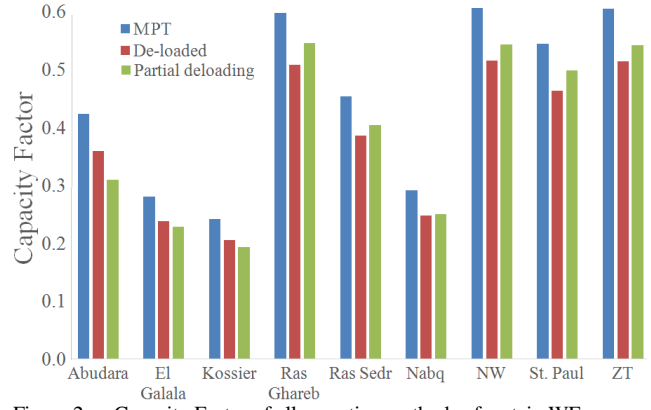| WTG Component	Failure rate λ Failure/year	Repair rate μ Hours	Unavailability Hours
Tower	0.006	104.1	0.713
Blades/Pitch	0.052	91.6	5.43
Gearbox	0.045	256.7	13.17
Generator	0.021	210.7	5.05
Converters	0.067	106.6	8.15
Controllers	0.05	184.6	10.53
Transformer	0.02	200	4.56
Yaw system	0.026	259.4	7.69
Brake system	0.005	125.4	7.16
Sensors	0.054	49.4	3.04

Figure 2   Capacity Factor of all operation methods of certain WFs

Sample data for certain conventional plants are depicted in Table III. Conventional units' reliability is represented by two-state model to mitigate computational efforts. However, an independent state transition time series array is generated for each unit within each simulation sample. Likewise, state transition arrays are also generated for transformers and transmission lines.

The lack of reliability data of transformers and transmission lines implied three assumptions: 1) transmission lines failure and repair rates are similar for the same transmission voltage level, 2) all transformers have the same failure and repair rates, 3) other system components are assumed to be healthy all the time. These assumptions will not deeply affect the relevance of obtained results since this paper mainly compares between pre and post WFs integration cases.

The evaluation of load points and overall system reliability is based on the methodology offered in [20]. However, taking into consideration the grid complexity (65 buses and 56 transmission lines), the maximum considered number of possible paths to feed certain load point is 10 paths.

The selected load points are divided into four categories as in Table IV. The expression 'Higher WFs feed' means that these points' demands are covered by high number of paths fed by WFs (i.e. 7 paths out of 10). Meanwhile, the high and low customers' number points are evenly supplied by WFs and conventional plants to highlight only the influence of customer count. Keep in mind that, in base case, load points are fed from conventional units only and sometimes number of paths is less than 10. An illustrative example for the applied 'paths' concept is depicted in Fig. 5. Points characterized by high number of customers have slightly higher feed from conventional units compared to WFs, and low-customers points have balanced feed. The approximate number of customers at each load point is assumed to be proportional to the population density [21]. The constant of proportionality is the total number of customers in the system.

Two indices from first hierarchical level, as well as CAIDI and CAIFI from third hierarchical level are estimated [22]. All indices are evaluated without, and with WFs integration (with former conventional capacity and also after replacement) plus the testing of the three highlighted operation methods (only for LOLE and LOEE). LOEE is evaluated using a modified method, where the load demand failures are obtained by subtracting the chronological load array from the available aggregate generation. Actual load chronological array is used to

generate a different load array in each sample year through Weibull probability function. Thus, the seasonal natures of load demand and wind power production are synchronized. On the contrary, standard method classifies system load into several levels where each level has its own annual occurrence probability (AOP). Egyptian grid load levels AOP are included in Fig. 4 in the left corner (average load levels are highlighted). It is worth mentioning that, the simulation process for 1000 samples, continued for 43 hours using a 2.53 GHz core-i3 CPU and 4 GB RAM DDR3.

B. Results

1) Impact of conventional capacity replacement

The results of load points that belong to the same category are combined together for simplicity and to get a wider view (e.g., CAIDI indices of load points of each category are aggregated in one average value). Results reveal that WFs integration does not have positive or negative impact all the time. But, the influence is affected by the nature of load point. For example, in first category CAIDI slightly increased after WFs integration before and after replacement as depicted in Fig. 6. This return

to shutting down some conventional units, hence the loss of demand probability is higher as this category counts more on conventional generation. On the contrary, in the third category, WFs integration reduced CAIDI by 2 hours (improved by 6% for high density customers regions). Nevertheless, conventional plant retirement ruined CAIDI by 16.7%. Likewise, the load points which count on WFs generation suffered worsened index especially, after conventional units' displacement (i.e., increased by 13.7%). However, the difference between pre and post replacement almost vanishes at lower density customer points. Only a minor improvement occurred since CAIDI is shortened by 90 minutes compared to base case. Most of the realized drawbacks are normal consequences for WS intermittency. Switching to CAIFI results displayed in Fig. 7, the impact of WFs integration is minor. This returns to the high reliability of WTGs which are available 98% from the year. Thus, the interruptions caused by their unhealthy states are very limited and interruptions are mainly caused by conventional units. This is insured by ASAI (Annual system availability index) results which are not fully included in this paper.
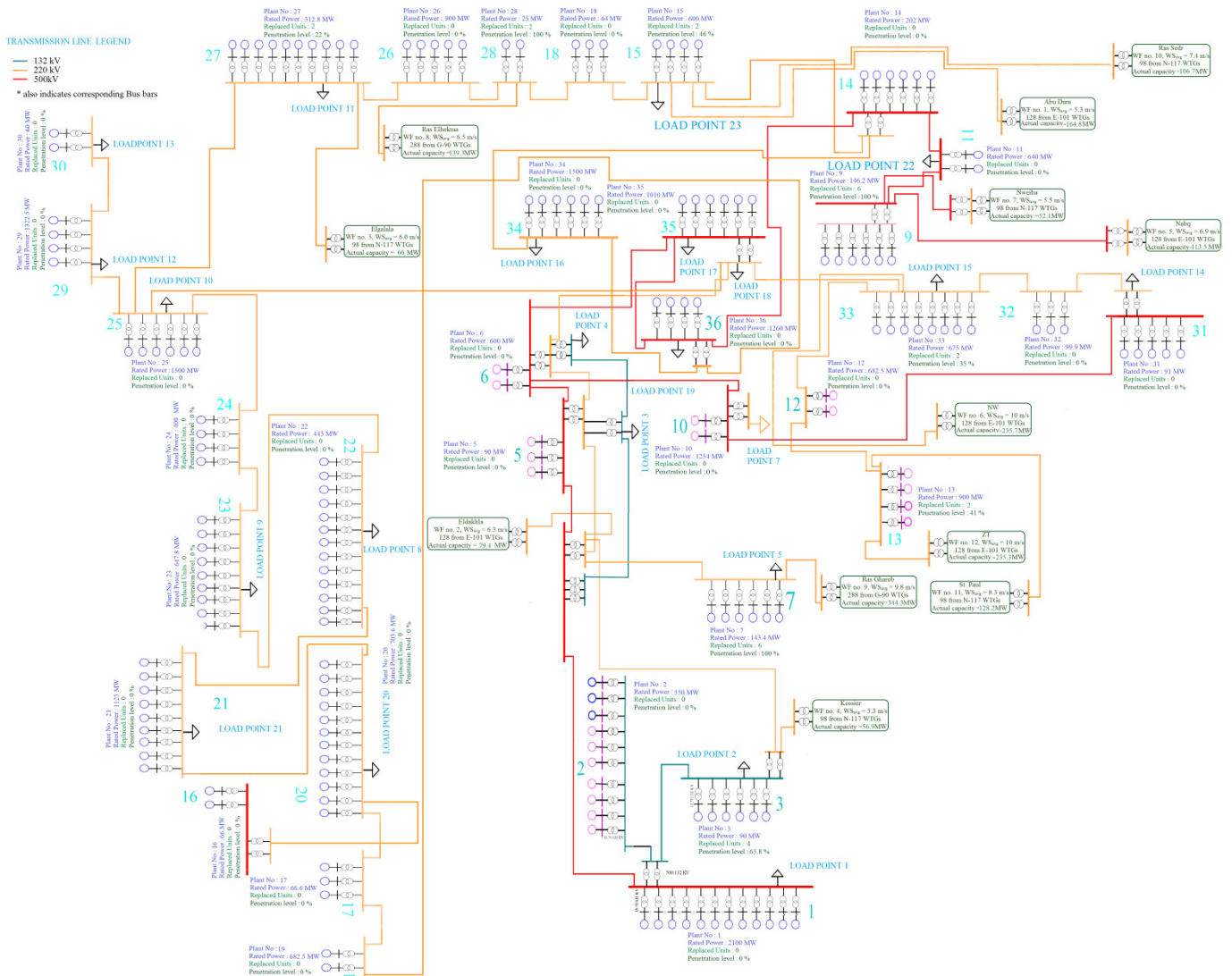

Figure 3 Egyptian grid composite single-line diagram before and after WFs integration (i.e., conventional generation retirement)

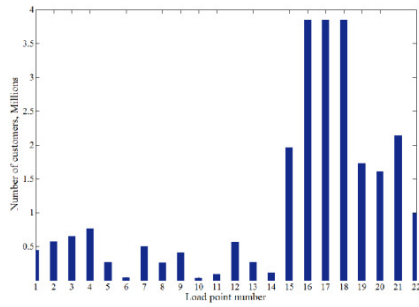| Load level, GW	AOP, %
17.30	0.1
16.84	0.4
16.37	1.2
15.91	2.4
15.45	4.5
14.99	5.0
14.52	4.1
14.06	5.0
13.60	7.3
13.14	6.8
12.67	7.1
12.21	9.5
11.75	12.1
11.29	11.9
10.82	9.9
10.36	8.2
9.90	3.2
9.43	0.8
8.97	0.2
8.51	0.1

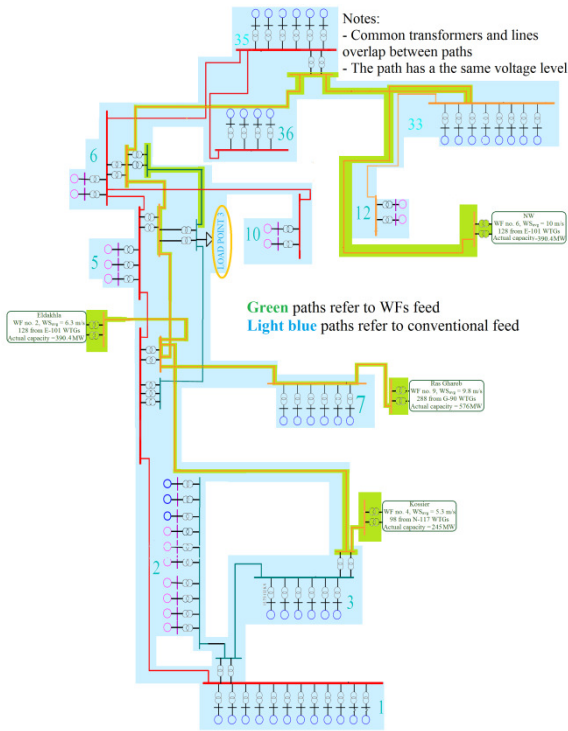Figure 4 AOP of major load levels and customer density at the main load points

Figure 5 Example for 'paths' method used to estimate load points' reliability indices

The deviations after WFs integration are also minor. It should be highlighted that, the WF is considered unavailable, from ASAI point of view, when the WF output is below its estimated actual capacity. The lowest ASAI occurs at fourth category with 89.6%. This is expected since low customers density points are always in remote locations. Thus, generation alternatives are limited and system unavailability risk is higher. Limited variations in estimated indices after conventional units' retirement refer to an acceptable replacement procedure and acceptable CF estimation method. Moreover, it insures that WFs development to feed rural sections is an adequate solution. It is worth mentioning that, more than 40% from Egyptian grid conventional units are relatively old therefore, they have low MTTF. This is emphasized in the results of first hierarchical indices which are discussed in the next subsection.

2) Impact of WTG operation method

Results highlight the impact of WSs conditions and WTG integrated operation algorithm. First of all, the relatively high base LOEE value found in Table V is not surprising, especially, when the 'real recorded' value in 2012 is considered, namely, 70 GWh [23]. The WFs 9% added (i.e., before replacements) capacity solidly improved LOEE by 98% even from Standard method point of view. Generally, Chronological method is always more optimistic by about 50% from standard (e.g., 56 GWh using Standard method and 25 GWh using Chronological one in Base case). Conventional units' retirement caused average increase in LOEE by 3.3 times compared to pre-retirement cases (e.g., at MPT; 0.75 enlarged to 2.46 GWh). However, evaluating LOEE using the proposed modified method has dramatically alleviated the former value.

TABLE III. REAL FAILURE DATA FOR SOME PLANTS IN EGYPTIAN GRID

Plant name, no. and type	MTTF, hours	MTTR, hours
Talkha, no. 20 in Fig. 2	7963	797
Steam, 2 units)	8164	596
Nubirua, no. 25 in Fig. 2 Gas, 4 units	6982	1778
	6859	1901
	7174	1586
	7376	1384
North Cairo, no. 34 in Fig. 2 Steam, 3 units	6684	2076
	6789	1971
	7507	1253

TABLE IV. SELECTED LOAD POINTS CATEGORIES

Category	Description	Load points' numbers
1	Higher conventional feed	21, 20, 8
2	Higher WFs feed	4, 18, 23
3	High customers no.	18, 21, 15
4	Low customers no.	6, 10, 14

TABLE V. SYSTEM INDICES RESULTS

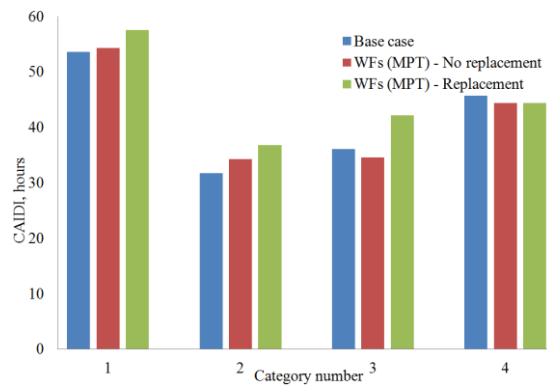| Index	LOLE	LOEE (GWh/year)	
Case study	(hours/year)	Standard	Chronological
Base case	55.88	55.97	24.55
WFs integrated -No replacements			
MPT	1.01	0.75	0.35
De-loaded	1.99	1.59	0.72
Partially de-loaded	1.98	1.598	0.72
WFs integrated -After replacements			
MPT	3.07	2.46	1.17
De-loaded	5.77	4.92	2.26
Partially de-loaded	5.82	4.93	2.26

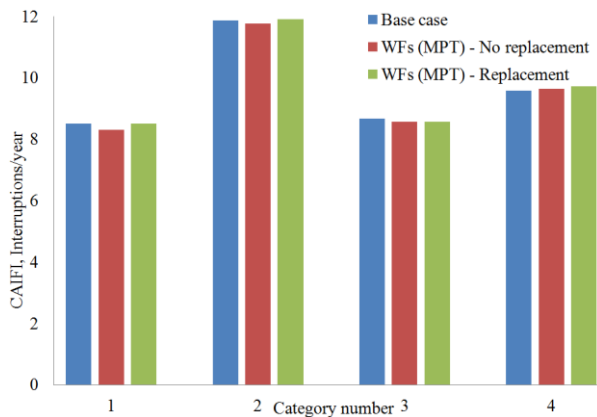Figure 6 CAIDI for the selected categories in all cases studies

Figure 7 CAIFI for the selected categories in all cases studies

Results also reveal the considerable impact of the good matching between WTG type and WF location. Likewise, LOLE index insured the same performance with almost the same ratios. The impact of operation algorithm is clearer in LOEE results. For example, MPT achieved the best results as expected in all cases. The MPT superiority is always in the range of 50%. Meanwhile, the two frequency support methods have minor deviations between each other. This might return to the homogeneous WS conditions in WFs locations. In other words, WS averages are evenly distributed between low and high levels among all sites. Thus, partial de-loading is preferred in locations of high and moderate WS conditions.

VII. CONCLUSIONS

This paper applies an innovative and detailed reliability multi-state model for WTG to build a WF reliability model including WS propagation influence and physical configuration of WTG inside the WF terrain. The WF comprehensive model is implemented to estimate the influence of frequency support algorithms on capacity factor and system reliability. Frequency support algorithms caused moderate reduction for capacity factors. However, the difference between the two support algorithms is noticeable in regions of good WS conditions. Thus, WS nature in WF location determines the favorite frequency support algorithm between partial de-loading and de-loading. The reliability indices analysis proved that wind energy integration solidly mitigated Standard LOEE. The improvements are clearer in the Modified LOEE. The operation method has a relatively minor impact on LOEE value.

REFERENCES

[1] B. K. Subramanian, A. B. Attya and T. Hartkopf, "Novel wind turbine reliability model- Implementation to estimate wind farms capacity credit," in IEEE 16th ICHQP, Bucharest, 2014.

[2] International Energy Agency, "World Energy Outlook,", Paris, 2012.

[3] X. Wang, J. Zhang, C. Jiang, D. L. L. Yu and Y. Weng, "Reliability assessment of wind farm active power based on sequential monte-carlo method," The International Journal of Energy Engineering, vol. 3, p. 122–129, 2013.

[4] A. Ghaedi, A. Abbaspour, M. Fotuhi-Firuzabad and M. Moeini-Aghtaie, "Reliability evaluation of a composite power system containing wind and solar generation," in IEEE 7th International Power Engineering and Optimization Conference, Langkawi, 2013.

[5] H. Kim, C. Singh and A. Sprintson, "Simulation and estimation of reliability in a wind farm considering the wake effect," IEEE Trans. on Sustainable Energy, vol. 3, no. 2, pp. 274 - 282, 2012.

[6] K. Brokish and J. Kirtley, "Pitfalls of modeling wind power using Markov chains," in IEEE Power systems conference and exposition, Seattle, 2009.

[7] P. Kundur, Power System Stability and Control, 1994: McGraw-Hill Inc., New York.

[8] J. Ekanayake and N. Jenkins, "Comparison of the response of doubly fed and fixed-speed induction generator wind turbines to changes in network frequency," IEEE Transactions on Energy Conversion, vol. 19, no. 4, pp. 802-812, 2004.

[9] A. B. Attya and T. Hartkopf, "Control and quantification of kinetic energy released by wind farms during power system frequency drops," IET Renewable Power Generation, vol. 7, no. 3, 2013.

[10] A. B. Attya and T. Hartkopf, "Wind turbine contribution in frequency drop mitigation – Modified operation and estimating released supportive energy," IET journal of Generation, Transmission and Distribution, 2013, http://digital-library.theiet.org/content/journals/10.1049/iet-gtd.2013.0512..

[11] T. Ackermann, Wind power in power systems, John Wiley & sons Ltd, 2005.

[12] R. de Almeida and J. Peas Lopes, "Participation of Doubly Fed Induction Wind Generators in System Frequency Regulation," IEEE Transactions on Power Systems , vol. 22, no. 3, pp. 944-950, 2007.

[13] C.-C. Le-Ren and Y. Yao-Ching, "Strategies for Operating Wind Power in a Similar Manner of Conventional Power Plant," IEEE transactions on energy conversion, vol. 24, no. 4, pp. 926-934, 2009.

[14] A. B. Attya and T. Hartkopf, "Wind energy in Egypt- Capacity assessment and analyzing penetration impact on grid frequency," in IEEE 4th International conference on power engineering, energy and electrical drives, Istanbul, 2013.

[15] M. Parker and O. Anaya-Lara, "Cost and losses associated with offshore wind farm collection networks which centralise the turbine power electronic converters," IET Journal of Renewable Power Generation, vol. 7, no. 4, pp. 390-400, 2013.

[16] A. B. Attya and T. Hartkopf, "Wind turbines support techniques during frequency drops — Energy utilization comparison," AIMS Energy Journal, vol. 2, no. 3, 2014.

[17] Y.-S. Juang, S.-S. Lin and H.-P. Kao, "A knowledge management system for series-parallel availability optimization and design, Expert Systems with Applications," vol. 34, no. 1, pp. 181-193, 2008.

[18] A. T. W. Schlez, "Wind farm siting and layout design," [Online]. Available: http://www.wwindea.org/technology/ch02/en/2 4 2.html.

[19] S. Emeis, Atmospheric Physics for Wind Power Generation, Springer, 2013.

[20] A. B. Attya, Y. G. Hegazy and M. A. Mostafa, "Evaluation of system reliability using seasonal and random operation techniques," in IEEE Power Engineering Society General Meeting, Pittsburgh, 2008.

[21] R. Billinton, Reliability assessment of electrical power systems using Monte Carlo methods, Springer, 1994.

[22] T. Brinkhoff, "City Population," 2014. [Online]. Available: http://www.citypopulation.de/Egypt-Cities.html.

[23] Euro-Mediterranean energy market integration project, "Overview of the power systems of the Mediterranean basin," April 2010. [Online]: http://ec.europa.eu/energy/international/studies/doc/2010_04_medring_vol 1.pdf.